CrossMark

FEBS openbio

FEBS

ELSEVIER

Phenylalanine 664 of dipeptidyl peptidase (DPP) 7 and Phenylalanine 671 of DPP11 mediate preference for P2-position hydrophobic residues of a substrate[☆]

Shakh M.A. Rouf[a], Yuko Ohara-Nemoto[a], Toshio Ono[a], Yu Shimoyama[b], Shigenobu Kimura[b], Takayuki K. Nemoto[a,*]

[a]Department of Oral Molecular Biology, Course of Medical and Dental Sciences, Nagasaki University Graduate School of Biomedical Sciences, 1-7-1 Sakamoto, Nagasaki 852-8588, Japan
[b]Division of Molecular Microbiology, Iwate Medical University, 2-1-1 Nishitokuda, Yahaba-cho 028-3694, Japan

ARTICLE INFO

ABSTRACT

Dipeptidyl peptidases (DPPs) are crucial for the energy metabolism in *Porphyromonas gingivalis*, a Gram-negative proteolytic and asaccharolytic anaerobic rod causing chronic periodontitis. Three DPPs, DPPIV specific for Pro, DPP7 for hydrophobic residues and DPP11 for Asp/Glu at the P1 position, are expressed in the bacterium. Like DPP7, DPP11 belongs to the S46 protease family, and they share 38.7% sequence identity. Although DPP11 is preferential for hydrophobic residues at the P2 position, it has been reported that DPP7 has no preference at the P2 position. In the present study, we defined the detailed P2 substrate preference of DPP7 and the amino acid residue responsible for the specificity. DPP7 most efficiently hydrolyzed Met-Leu-dipeptidyl-4-methylcoumaryl-7-amide (MCA) carrying hydrophobic residues at the P1 position with k_{cat}/K_m of 10.62 ± 2.51 μM^{-1} s^{-1}, while it unexpectedly cleaved substrates with hydrophilic (Gln, Asn) or charged (Asp, Arg) residues. Examination with 21 dipeptidyl MCA demonstrated that DPP7-peptidase activity was dependent on hydrophobicity of the P2- as well as P1-position residue, thus it correlated best with the sum of the hydrophobicity index of P1- and P2-amino acid residues. Hydrophobicity of the P1 and P2 positions ensured efficient enzyme catalysis by increasing k_{cat} and lowering K_m values, respectively. Substitution of hydrophobic residues conserved in the S46 DPP7/DPP11 family to Ala revealed that Phe664 of DPP7 and Phe671 of DPP11 primarily afforded hydrophobic P2 preference. A modeling study suggested that Phe664 and Gly666 of DPP7 and Phe671 and Arg673 of DPP11 being associated with the P2- and P1-position residues, respectively, are located adjacent to the catalytic Ser648/Ser655. The present results expand the substrate repertoire of DPP7, which ensures efficient degradation of oligopeptides in asaccharolytic bacteria.

1. Introduction

Porphyromonas gingivalis, a Gram-negative proteolytic and asaccharolytic anaerobe, is a major causative organism of chronic periodontitis [1,2], which leads to loss of permanent teeth [3–5] and, thus, affects quality of life, especially in elderly individuals [6]. Much attention has recently been paid to this bacterium because of its close relationship with systemic diseases including cardiovascular disorders [7], decreased kidney function [8] and rheumatoid arthritis [9].

P. gingivalis does not ferment glucose, cellobiose, lactose or sucrose [10], while it requires proteinaceous substrates as carbon and energy sources. Amino acids are incorporated into the bacterial cells mainly as dipeptides, not as free amino acids [11,12]. Therefore, dipeptidyl-peptidases (DPPs) that release dipeptides by cleavage of the penultimate peptide bond (P1 position) from the N-terminus of an oligopeptide are crucial for bacterial metabolism [13–15]. If dipeptides with any sequences can be released by DPPs, it appears to be advantageous for energy production by the bacterium.

To date, three DPPs belonging to serine protease family have been identified to be expressed as cell-bound forms in *P. gingivalis*. The S9B-family peptidase DPPIV (Uniprot ID, B2RKU3/MEROPS ID, MER004211) is specific for Pro at the P1 position [13] and basically accepts any residues at the N-terminus position (P2 position) [16], though bulky P2-position residues are optimal for the activity [17]. DPP7 (B2RKV3/MER014366) is highly preferential for hydrophobic
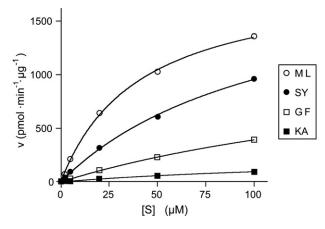
Fig. 1. Substrate dependence of the DPP7 activity. Activities of DPP7 were measured with Met-Leu-, Ser-Tyr-, Gly-Phe- and Lys-Ala-MCA. Representative data are shown from five separate experiments.

Fig. 2. Hydrolyzing activity of DPP7. The dipeptidyl peptidase activity of recombinant DPP7 was determined using 21 dipeptidyl MCA substrates (20 μM). Values are shown as the mean ± SD ($n = 3$).

Fig. 3. Amino acid preference of DPP7 at the P1 and P2 positions. The log of specific activities of DPP7 for dipeptidyl MCA (Fig. 2) were plotted against hydrophobicity index (H.I.) of amino acid at (A) P1-, (B) P2- and (C) the sum of the P1- and P2-position residues at pH 7. Solid lines show fitted lines for the correlation between the activity and H.I. [$R = 0.536$, $p = 0.01$ in (A); $R = 0.402$, $p = 0.07$ in (B), and $R = 0.738$, $p = 0.0001$ in (C)]. Six substrates (ML, SY, GF, KA, LD and LE), of which k_{cat} and K_m were determined (Table 1), are indicated as closed circles. (D) H.I. of P1, P2 and P1 + P2 residues of substrates.

D

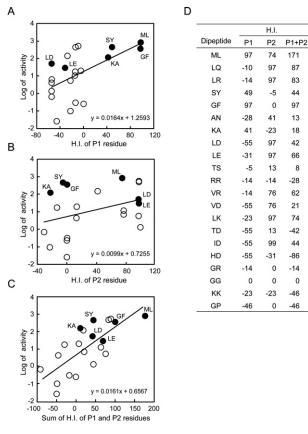| Dipeptide	H.I.		
	P1	P2	P1+P2
ML	97	74	171
LQ	-10	97	87
LR	-14	97	83
SY	49	-5	44
GF	97	0	97
AN	-28	41	13
KA	41	-23	18
LD	-55	97	42
LE	-31	97	66
TS	-5	13	8
RR	-14	-14	-28
VR	-14	76	62
VD	-55	76	21
LK	-23	97	74
TD	-55	13	-42
ID	-55	99	44
HD	-55	-31	-86
GR	-14	0	-14
GG	0	0	0
KK	-23	-23	-46
GP	-46	0	-46

residues at the P1 position and its activity appears to be not affected by the P2-position residue [14]. Our recent study indicated that DPP7 shows a rather broad specificity, in which moderate hydrolysis of Leu-Arg- and Leu-Asp-MCA was not simply explained by the hydrophobic P1 preference [18]. In addition to these DPPs, we recently found DPP11 (B2RID1/MER34628) that is specific for Asp/Glu and possesses a hydrophobic P2 preference [15]. DPP7 and DPP11 share sequence similarity, and hence, both belong to the S46 peptidase family. The optimum pH of DPPIV, DPP7 and DPP11 are pH 7.5 [13], 7–8 [14] and 7.0 [15], respectively, which seem to be adapted to its inhabiting environment.

Substitution analysis of conserved residues in respective S46 members demonstrated that Arg673 of DPP11 is primarily important for recognition of the P1 residue, Asp or Glu [15]. Similarly, Gly666 that is conserved in DPP7 and equivalent to Arg673 of DPP11 mediates P1 preference for bulky and hydrophobic residues [18].

In addition to above three DPPs, the gene (PGN_1645) encoding putative DPPIII (YP_004510152.1) has been found in *P. gingivalis* ATCC 33277 [19]. Although DPPIII has been considered to exclusively exist in eukaryotes [20], bacterial DPPIII has recently reported in *Bacteroides thetaiotaomicron* [21]. *B. thetaiotaomicron* DPPIII most potently hydrolyzes Arg-Arg-2-naphthylamide as does eukaryotic DPPIII [20]. However, its N-terminal sequence indicates its localization in the cytosol [21], and hence, bacterial DPPIII may not participate
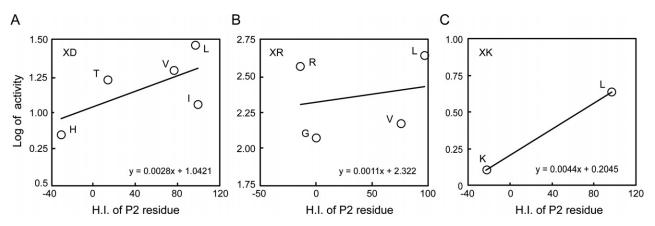
in the degradation of environmental peptides, but be responsible for degradation of cytosolic substrates.

In the present study, we defined detailed P1 and P2 preferences of DPP7 using a preparation free from other *P. gingivalis* peptidases. For this purpose, we expressed active recombinant DPP7 and its single substitution mutants in *Escherichia coli*. Measurements of activity with a series of dipeptidyl 4-methylcoumaryl-7-amide (MCA) demonstrated that DPP7 does not simply prefer hydrophobic residues at the P1 position, while its hydrolyzing activity is influenced by both P1- and P2-amino acids. Substitution experiments suggested that Phe664 of DPP7 and equivalent Phe671 of DPP11 were responsible for recognition of the P2-position hydrophobic residue of substrates.

2. Materials and methods

2.1. Materials

pQE60 from Qiagen was used as an expression and cloning vector. Restriction enzymes and DNA-modifying enzymes were purchased from Takara Bio and New England Biolabs, while KOD Plus DNA polymerase came from Toyobo (Tokyo, Japan). Oligonucleotide primers were from FASMAC (Atsugi, Japan). Commercially unavailable dipeptidyl-MCA substrates were prepared from peptidyl-MCA (0.4 mM) through digestion with 0.3 μg of thermolysin from *Bacillus thermoproteolyticus rokko* (Sigma), bovine trypsin (Sigma) or GluV8 [22] in 10 mM sodium borate (pH 8.0) and 2 mM CaSO₄ containing 0.005% (v/v) Triton-X100 (100 μl) at 37 °C for 4 h: Leu-Arg-, Val-Arg-, Leu-Lys-, Ala-Arg-, Ala-Asn- and Leu-Gln-MCA were

Fig. 4. Amino acid preference of DPP7 at the P2 position. The log of specific activities of DPP7 for dipeptidyl MCA with identical P1 residues were plotted against H.I. at (A) the P2-position residue of Xaa-Asp-, (B) Xaa-Arg- or (C) Xaa-Lys-MCA. Solid lines show fitted lines for the correlation between the specific activity and hydrophobicity index [$R = 0.680$, $p = 0.320$ in (A); $R = 0.641$, $p = 0.244$ in (B)].

produced from acetyl (ac)-KTKQLR-, benzyloxycarbonyl (Z)-VVR-, *t*-butyloxycarbonyl (boc)-VLK-, boc-QAR-, AAN and Z-LLQ-MCA by pretreatment with thermolysin, respectively; Gly-Arg-, Lys-Lys-, Thr-Asp-, Val-Asp-, Ile-Asp- and His-Asp-MCA from boc-IEGR-, boc-EKK-, ac-IETD-, ac-DEVD-, ac-VEID- and ac-IEHD-MCA with GluV8, respectively. Leu-Asp-, Leu-Glu- and Z-LLQ-MCA were synthesized by Thermo Fisher Scientific (Ulm, Germany) and TORAY (Tokyo, Japan). Met-Leu-, Arg-Arg-, Gly-Phe-, Ser-Tyr-, Thr-Ser- and Gly-Gly-MCA were obtained from Bachem (Dubendorf, Switzerland). Other MCA peptides were from the Peptide Institute Inc. (Osaka, Japan).

2.2. Construction of expression plasmids

P. gingivalis ATCC 33277 genomic DNA was purified as previously reported [23]. A DNA fragment encoding DPP7 (PGN_1479, Met3-Ile712 was amplified by PCR with a set of primers [5′-GACTGCT*AGATCT*CAAATGAAATTAAAAAGTATTC and 5′-GGCGAAT*AGATCT*GATCAACTTCAGCTC (*Bgl*II sites indicated by italics)], digested with *Bgl*II, and then cloned into the *Bam*HI site of pQE60. Construction of the expression plasmid for *P. gingivalis* DPP11 was previously reported [18].

2.3. Numbering of amino acids residues of DPP7 and DPP11

Amino acid residues were numbered from Met1 of DPP7 (712 residues) and DPP11 (720 residues). Accordingly, Phe637, Ser648, Leu659, Phe664, Asp665, Gly666 and Leu693 of DPP7 are equivalent to Phe644, Ser655, Leu666, Phe671, Asp672, Arg673 and Leu700 of DPP11, respectively.

2.4. In vitro mutagenesis

In vitro mutagenesis was performed using a PCR technique with appropriately mutated primers. Phe69, Leu83, Val200, Phe226, Phe229, Phe637, Leu659, Phe664 and Leu693 of DPP7 and Phe644, Leu666, Phe671 and Leu700 of DPP11 were substituted with Ala. All mutations were confirmed by nucleotide sequencing.

2.5. Expressions of P. gingivalis DPP7 and DPP11 in E. coli

E. coli XL1-Blue carrying a pQE60-derived expression plasmid was cultured in Luria–Bertani broth containing 75 μg/ml of ampicillin at 37 °C overnight. Protein expression was induced by dilution of the culture with two volumes (800 ml in a 3-L baffled flask) of the broth containing 0.2 mM isopropyl β-D-thiogalactopyranoside and incubation at 30 °C for 4 h. Bacterial cells were harvested by centrifugation

and lysed with lysis/washing buffer (20 mM Tris–HCl, pH 8.0, 0.1 M NaCl containing 10 mM imidazole) to which 0.4 mg/ml of lysozyme and 10 μg/ml of leupeptin had been added. Recombinant proteins were recovered in the cell lysate fraction and then purified by an affinity chromatography with Talon metal affinity resin (Clontech Lab. Inc., Palo Alto, CA) according to the manufacturer's protocol, except that 10 mM imidazole was included in the lysis/washing buffer. After extensive washing, bound proteins were eluted with 0.1 M imidazole (pH 8.0) containing 10% (v/v) glycerol. Expressed DPPs were stored at −80 °C until used.

2.6. Hydrolyzing activity toward dipeptidyl MCA

Recombinant DPPs (50 ng of DPP7 and 5 ng of DPP11) were incubated with 20 μM dipeptidyl MCA in 200 μl of reaction solution composed of 50 mM sodium phosphate (pH 7.0) and 5 mM EDTA at 37 °C for 1 h. Fluorescence intensity was measured with excitation at 380 nm and emission at 460 nm with a Fluorescence Photometer F-4000 (Hitachi). To determine the enzymatic parameters, different concentration of dipeptidyl MCA (0.5–100-μM) were incubated with wild type and single amino acid mutated DPP7. The results were analyzed by nonlinear regression curve fitting to the Michaelis–Menten equation using a GraphPad Prism software program (San Diego, CA, USA). Averages and standard deviations were calculated from three to nine independent measurements.

2.7. Homology modeling

Models of DPP7 and DPP11 were built using an automated homology modeling program EsyPred3D [24], with the known structure of GluV8 chain 'A' (2o8I) [25] as a template. Obtained structures were visualized using PyMOL.

3. Results

3.1. Substrate specificity of P. gingivalis DPP7

Recombinant DPP7 was expressed in *E. coli* and purified to homogeneity with an apparent molecular mass of 70 kDa (data not shown). Substrate specificity of DPP7 was compared on six dipeptidyl MCA substrates, and catalytic rate constant (k_{cat}) and K_m were determined from the concentration dependence of the reaction, such as shown in Fig. 1. Enzymatic parameters are listed in Table 1. DPP7 showed larger specificity constants (k_{cat}/K_m) for the substrates carrying hydrophobic residues [Leu, Tyr and Phe with hydrophobicity indexes (H.I.) [26]

```
                              ▼                                    ⇩                      ↓        *
PgDPP7     1 MQMKLKSILLGAALLLGASGVAKADKGMWLLNELNQENLDRMELGFTLPLDSLYSFDKPSIANAVVIFGGGCTGITVSDQGLIFTNHHC   90
PgDPP11    1 MKKRLLLPLFAAL-CLSQIAH--ADEGMWLMQQLGRKYAQM-KERGLKMKEYDLYNPNGTSLKDAVVLFDGGCTGEVVSDRGLVLTNHHC   86
                              ▲   GmW                           G                   a     GC    S  GL  TNHHC

PgDPP7    91 GYGAIQSQSTVDHDYLRDGFVSRTMGEELPIPGLSVKYLRKIVKVTDKVEGQLKGITDEMERLRKAQEVCQELAKKENADENQLCI----  176
PgDPP11   87 GYDMIQAHSTLEHNYLENGFWAMREADELPNKDISVVFIDKIEDVTDYVKKELKAIKDPNSMDYLSPKYLQKLADKKAGKNFSAKNPGLS  176
                       S        G   A     E                   T

                           *        ↓                     ⇩     ⇩
PgDPP7   177 VE--PFYSNNEYFLIVYDVFKDVRMVFAPPSSVGKFGGDTDNWMWPRHTGDFSVFRVYAGADNRPAEYSKDNKPYKPVYFAAVSMQGYKA  264
PgDPP11  177 VEIKAFYGGNLYLMFTKKTYTDVRLVGAPPSSIGKFGADTDNWIWPRHTGDFSIFRIYADKNGNPAPYSEDNVPLKPKRFFNISLGGVQE  266
                G      l        D R V aP   G Gg DN   PR t D    R Y    PA    n p           G

PgDPP7   265 DDYAMTIGFPGSTDRYLTSWGVEDRIENENNPRIEVRGIKQGIWKEAMSADQATRIKYASKYAQSANYWKNSIGMNRGLARLDVIGRKRA  354
PgDPP11  267 NDYAMIMGFPGTTHRYFTASEVDEWKSIDNDIRIRMRDIRQGVMLREMLADPQIKIMYSAKYAASQNAYKRAIGANWAIKTRGLRQNKQA  356
                g      G PG T R                                            N K    G              K

PgDPP7   355 EERAFADWIRKNGKSAVYGDVLSSLEKAYKEGAKANREMTYLSETLFGGTEVVRFA----QFANALATNP-DAHAGILKSLDDKY-----  434
PgDPP11  357 MQDRLIAWGAKQGTPR-YEEAVHEIDATVAKRADLRRRYWMIEEGIIRGIEFARSPIPTEDETKALQGNDASARKEAIDKIRTRYSKFAN  445

PgDPP7   435 KDYLPSLDRKVLPAMLDIVRRRIPADKLPDIFKNVIDKKFKGDTKKYADFVFDKSVVPYSDKFHAMLKSMDKEKFAKAIEKDPAVELSKS  524
PgDPP11  446 KDYSAEVDKKVAVAMLTEYLKEIPYENLPLHLRLVKDR-FAGDVQAYVDDIFARSVFGSEAQFDAFAAVPSVEKLAE----DPMVLFASS  530
                                                                                              Dp

PgDPP7   525 VIAAARAIQADAMANAYAIEKGKRLFFAGLREMYPGRALPSDANFTMRMSYGSIKGYEPQDGAWYNYHTTGKGVLEKQDPKSDEFAVQEN  614
PgDPP11  531 VFDEYRKLYNELRPYDDPILRAQRTYIAGLLEMDGDQDQFPDANLTLRFTYGQVKGYSPRDNVYYGHQTTLDGVMEKEDPDNWEFVVDPK  620
                                                PDAN T R  G                Tt      K                p

                          ↓                        *        ↓       ↓    +                            ↓
PgDPP7   615 ILDLFRTKNYGRYAE-NGQLHIAFLSNNDITGGNSGSPVFDKNGRLIGLAFDGNWEAMSGDIEFEPDLQRTISVDIRYVLFMIDKWGQCP  703
PgDPP11  621 LKAVYERKDFGRYADRSGRMPVAFCATTHTTGGNSGSPVMNANGELIGLNFDRNWEGVGGDIQYLADYQRSIIVDIRYVLLVIDKVGGCQ  710
                                       F    D tGGNSGSP   G l G FD              R   VD Ry L

GluV8                  164 TTGGNSGSPVFNEKNEVIGIHWGGVP 189

PgDPP7   704 RLIQELKLI-  712
PgDPP11  711 RLLDEMNIVP  720
                L E
```

Fig. 5. Effects of the substitutions of conserved and hydrophobic residues on the DPP7 activity. (A) Amino acid sequences of *P. gingivalis* DPP7 and DPP11 are shown. Sequences of 263 members of the S46 family [16] and DPP11 from *P. endodontalis* [15] were compared, and the residues conserved in more than 95% (capital letters), 80% ≤ x < 95% (capital and italic letters) and 70% ≤ x < 80% (small letters) members are described below the sequences of DPP11 and DPP7. Conserved (closed arrows) and non-conserved (open arrows) hydrophobic amino acids were substituted with Ala. Stars indicate essential His89, Asp196 and Ser648 forming an active triad. Triangles indicate maturation cleavage sites producing mature DPP7 [14] and DPP11 [15]. A plus mark indicates Gly666 of DPP7 and Arg673 of DPP11 essential for P1-position recognition [15,18]. A homologous region of GluV8 (Thr164–Pro189) to the S46 family is described, and amino acids identical to either *P. gingivalis* DPP7 or DPP11 are underlined. (B) Activities of DPP7 and its mutants were measured with Met-Leu-, Leu-Arg- and Gly-Phe-MCA. Inset shows expanded data for F637A and F664A. Values are shown as the mean ± SD (n = 3). (C) The ratio of the activity for Gly-Phe-MCA to that for Leu-Arg-MCA is plotted.

of 97, 49 and 100, respectively], than those carrying a less hydrophobic residue, Ala (41), and hydrophilic residues, Asp (−55) and Glu (−31), at the P1 position. Furthermore, the k_{cat}/K_m values seemed to vary by the P2 residues, since H.I. of Leu in Met-Leu-MCA was comparable to Phe in Gly-Phe-MCA, whereas the figure for Met-Leu-MCA was 9-fold higher than that for Gly-Phe-MCA. We thus further compared the hydrolyzing activity of DPP7 with a number of substrates at a single concentration of 20 μM.

The DPP7 activities for 21 dipeptidyl MCA substrates exhibited a rather broad spectrum (Fig. 2), in contrast to the narrow specificity of DPPIV [13] and DPP11 [15]. Among the substrates examined, Met-Leu-MCA was most efficiently cleaved, as it carries one of the most hydrophobic residues (H.I. = 97) at the P1 position. Furthermore, DPP7 unexpectedly cleaved Leu-Gln- and Leu-Arg-MCA, despite the fact that they carry non-hydrophobic P1 residues. Subsequently, Ser-Tyr-, Gly-Phe-, Ala-Asn- and Lys-Ala-MCA were efficiently hydrolyzed with specific activities higher than 100 pmol min⁻¹ μg⁻¹. Thereafter, Leu-Asp-, Leu-Glu-, Thr-Ser- and Arg-Arg-MCA were cleaved with that

Table 1
Enzymatic parameters of *P. gingivalis* DPP7 for dipeptidyl MCA substrates.

Species	Substrate	K_m (µM)	k_{cat} (s^{-1})	k_{cat} /K_m (µM^{-1} s^{-1})
Wild type	Met-Leu-MCA	39.55 ± 15.95	393.65 ± 78.72	10.62 ± 2.51
	Ser-Tyr-MCA	102.86 ± 18.77	397.94 ± 41.62	3.92 ± 0.50
	Gly-Phe-MCA	292.70 ± 60.09	340.87 ± 60.30	1.17 ± 0.07
	Lys-Ala-MCA	154.40 ± 20.37	49.36 ± 9.05	0.32 ± 0.02
	Leu-Asp-MCA	19.36 ± 1.15	8.26 ± 0.11	0.43 ± 0.02
	Leu-Glu-MCA	62.06 ± 4.06	10.52 ± 0.35	0.17 ± 0.01
F664A	Met-Leu-MCA	106.56 ± 10.15	114.72 ± 6.24	1.08 ± 0.04

Enzymatic parameters (mean ± SD) of wild type and F664A DPP7 were obtained at least from three separate experiments.

higher than 10 pmol min^{-1} µg^{-1}; and Val-Arg-, Val-Asp-, Leu-Lys-, Thr-Asp- and Ile-Asp-MCA to lesser extents (>1 pmol min^{-1} µg^{-1}). The remaining substrates were scarcely hydrolyzed. These results indicated that DPP7 targeted the peptides not only with hydrophobic but also with hydrophilic (Gln and Asn), as well as charged (Arg, Lys, Asp and Glu) residues at the P1 position. In particular, it was notable that DPP7 hydrolyzed Leu-Gln-MCA 4.5-fold more efficiently than Lys-Ala-MCA, and that the presence of a hydrophobic side chain (Leu) at the P2 position was common in these hydrolyzed substrates. Accordingly, we further characterized the substrate specificity of DPP7 by taking into consideration the P2-position residues.

3.2. P1- and P2-position preferences of DPP7

The preference of DPP7 for hydrophobic P1 amino acids was confirmed using a plot of activity against the H.I. of amino acid residues (Fig. 3) in consistent with the previous study [14]. Moreover, a weak but positive correlation with the hydrophobicity of P2-position residues was observed, hence the DPP activity was best correlated with the sum of H.I. of the P1- and P2-position residues.

To clearly elucidate the influence of the P2-position residues, the H.I. values of P2-position residues were compared among dipeptidyl MCA carrying common P1 residues, *i.e.*, Asp, Arg or Lys (Fig. 4). In all cases, the activities for Xaa-Asp- (Xaa = Leu, Val, Ile, Thr or His), Xaa-Arg- (Xaa = Leu, Val, Arg or Gly) and Xaa-Lys-MCA (X = Leu or Lys) were proportional to the H.I. values of the P2-position residues, though the statistical significance of the correlations was higher than 0.05 due to the limited number of substrates available. Taken together, we concluded that the activity of DPP7 was dependent on hydrophobicity not only at the P1, but also at the P2 position. Accordingly, it was reasonably explained that Met-Leu-MCA possessing the highest H.I. value (173) was the best substrate for DPP7 (Figs. 2 and 3). Furthermore, these results revealed that the hydrophobic preference at the P2-position residue was a common characteristic of the S46 family, i.e., DPP7 and DPP11 [15].

An important role of the P2-position hydrophobicity in the DPP7 activity was also supported by the fact that small K_m values were commonly observed for the substrates carrying hydrophobic residues at the P2 position, i.e., Met-Leu-, Leu-Asp- and Leu-Glu-MCA (Table 1). To the contrary, large k_{cat} values were common for substrates carrying hydrophobic residues at the P1 position, i.e., Met-Leu-, Ser-Tyr- and Gly-Phe-MCA. Taken together, these results indicated that hydrophobicity of the P1- and P2-position residues contributed mainly an increase in k_{cat} and lowering of K_m values, respectively, in DPP7.
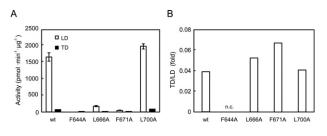
3.4. Phe644 defines hydrophobic P2 preference of DPP7

The hydrophobic P2 preference of DPP7 led us to suspect that hydrophobic residue(s) are involved in P2-position recognition, which may be conserved in S46 family members. Alignment of the amino acid sequences of all 264 members (MEROPS database, Release 9.6) [16] demonstrated that there are nine conserved hydrophobic

residues; with Leu83 and Phe664 completely conserved in all members; Trp29, Val200, Phe637, Leu693 and Leu705 highly conserved ($80\% \leq x < 95\%$); and Met28 and Leu659 relatively conserved ($70\% \leq x < 80\%$) (Fig. 5A). If any of these hydrophobic residues (Phe, Trp, Leu, Val and Met with H.I. values of 100, 97, 97, 76 and 74, respectively) truly participates in interactions with the P2 residue, then substitution to a less hydrophobic residue, Ala (H.I. = 41), may reduce the proteolytic activity. In particular, the reduction may be more significant for a substrate with a hydrophobic residue at the P2 position, whereas it may be limited for a substrate carrying a non-hydrophobic P2 residue. Thus, Leu-Arg-MCA (H.I. = 83 as the sum of 97 and −14 in the P2- and P1-position residues, respectively) and Gly-Phe-MCA (H.I. = 100 as the sum of 0 and 100, respectively) were selected as substrates possessing comparable H.I. values as the sum, but with values in contrast to the P1 position.

To test this assumption, six single substitution mutants (L83A, F664A, V200A, F637A, L693A, L659A) of nine conserved hydrophobic residues were constructed. Three residues, i.e., Met28, Trp29 and Leu705, were excluded from this analysis, because they are located near the N- or C-terminal edge of the molecule, and hence are unlikely to be involved in substrate recognition. We also prepared three additional Phe-to-Ala-substitution mutants (Phe69, Phe226 and Phe229, which are conserved less than 70%) as controls. As shown in Fig. 5B, the activities for Met-Leu-, Leu-Arg- and Gly-Phe-MCA of the mutants were consistently reduced as compared to the wild type (wt). The ratio of the activities for Gly-Phe-MCA to Leu-Arg-MCA was the highest in F664A (Gly-Phe/Leu-Arg = 4.62), followed by F637A (1.08), F659A (0.66) and L693A (0.60), while those values for the wt, F69A, L83A, V200A, F226A and F229A, were substantially lower (0.23–0.42) (Fig. 5C). These findings strongly suggest the involvement of Phe664 in hydrophobic P2 recognition. This mutation decreased specificity constant for Met-Leu-MCA through affecting both k_{cat} and K_m (Table 1). Even though involvement of Phe637 as well as Leu659 and Leu693 was also surmised, their effects seemed to be limited as compared to Phe664.

3.5. Phe671 defines hydrophobic P2 preference of DPP11

Because DPP11 as well as DPP7 shows hydrophobic P2 preference [15], we also investigated the amino acid residue(s) of DPP11 responsible for the P2 hydrophobic preference. Recombinant DPP11 was expressed in *E. coli* and purified to homogeneity with an apparent molecular mass of 80 kDa, as reported previously [18]. Two residues (Leu79 and Val202) of DPP11 were omitted from comparison after considering the above-described result for DPP7. Hence, four conserved and highly hydrophobic residues (Phe644, Leu666, Phe671 and Leu700) were substituted with Ala. Since either Asp or Glu was indispensable at the P1 position, we chose Leu-Asp- (H.I. of Leu = 97) and Thr-Asp-MCA (H.I. of Thr = 13) as substrates carrying P2 residues with contrast values for this assay. As shown in Fig. 6A, the hydrolyzing activity of Leu-Asp-MCA by DPP11 wt was much higher than that of Thr-Asp-MCA, reflecting the hydrophobic P2 preference of DPP11. Since L700A showed a comparable activity to wt, Leu700

Fig. 6. Effects of amino acid substitutions on DPP11. (A) Activities of DPP11 and its Ala-substitution mutants were measured with Leu-Asp- and Thr-Asp-MCA. (B) The ratio of the activity toward Leu-Asp- and Thr-Asp-MCA is plotted. n.c., Not calculated because of complete loss of activity. Values are shown as the mean $\pm$ SD ($n = 3$).
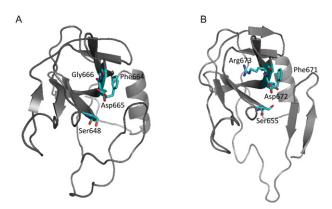

Fig. 7. Structural model of conserved C-terminal sequences of DPP7 and DPP11. Modeling of the three-dimensional structures of (A) DPP7 (Asp566-Met695) and (B) DPP11 (Asp572-Val702) was performed with an EsyPred3D program based on the structure of GluV8 (2o8l) [25]. Essential Ser648 of DPP7 and Ser655 of DPP11 and residues involved in the hydrolytic activity are indicated.

was excluded from possible residues required for substrate specificity. The activities of L666A and F671A were markedly decreased, and F644A completely lost activity toward both substrates. The ratio of the activities for Thr-Asp-MCA to Leu-Asp-MCA was the highest in F671A (Fig. 6B). Therefore, Phe671 of DPP11 probably interacts with the P2-position hydrophobic residue as observed in DPP7 (Fig. 5B). However, since disturbing the local conformation or secondary structure could cause the decrease in activity, another method, e.g., three-dimensional structure determination, would be necessary to confirm a direct interaction.

3.6. Modeling of substrate-binding sites of DPP7 and DPP11

The three-dimensional structures of the S46 family members DPP7 and DPP11 are yet to be established. Hence, we applied an automated homology modeling program, EsyPred3D [24], to examine the structural relationship between essential Ser648 and Phe664 involved in P2-residue recognition. In addition, it was considered important to examine the residue at position 666, because Arg673 in DPP11 equivalent to Gly666 of DPP7 is predicted to interact with a P1-position acidic residue [15], and Gly666 of DPP7 is required for optimal acceptance of a P1-position bulky and hydrophobic residue [18]. The modeling program automatically chose the specificity-determining C-terminal conserved region of the S46 family [18] using a scaffold template of the *Staphylococcus aureus* glutamyl endopeptidase GluV8 [25], which shows amino acid identity of 7.5% to DPP7 and 9.2% to DPP11 in the full sequence, and that of 15.7% to DPP7 and 16.2% to DPP11 in the modeled region. The topology of the active triad of GluV8, His51, Asp93 and Ser169, is identical to that of His89, Asp196 and Ser648 of DPP7, and residues 164–173 of GluV8 (numbering as mature form) [27] carrying active Ser169 shares sequence similarity with DPP7 and DPP11 (Fig. 5A). As a result, Asp566-Met695 of DPP7 and Asp572-Val702 of DPP11 were modeled based on the structure of GluV8. The model structure indicated that the tripeptidyl segments Phe664-Asp665-Gly666 (DPP7) and Phe671-Ap672-Arg673 (DPP11) are sterically adjacent to essential Ser648 and Ser655, respectively (Fig. 7). The importance of these segments was also indicated by complete conservation of Phe664/Phe671 and Asp665/Asp672 in the S46 family [16].

4. Discussion

Classification of DPPs from DPPI to DPP11 has generally been performed based on differences in substrate specificities [16], in which the P1-position residues seem to be most critical. The previous study on substrate specificity of *P. gingivalis* DPP7 had also focused on the P1 position, but was unable to refer to P2 position due to limited number of substrates used. Later in a review article, the authors noted that P2-position specificity of DPP7 should be carefully re-examined [28].

Even though DPP11 is specific for acidic amino acids, its proteolytic activity is also influenced by the hydrophobicity of the P2-position residues. For example, hydrolysis of Ile-Asp-MCA was 10-fold faster than that of His-Asp-MCA [15]. Moreover, the present findings revealed the hydrophobic P2 preference of DPP7 and, accordingly, DPP7 more preferably cleaves substrates with higher H.I. values of P1 and P2 residues. In fact, the similar tendency that a hydrophobic P2 preference of *P. gingivalis* DPP7 was also observed in the previous data [14], as N-terminal and subsequent residues of cleavable substrates had higher H.I. values [Phe-Leu-, Ala-Phe-, Ile-Ala-, Trp-Ala-, Gly-Phe- and Lys-Ile-β-naphthylamide hydrochloride (*p*NA) with 197, 141, 140, 138, 100 and 76, respectively], whereas those of un-cleavable peptides were relatively lower (Trp-His-, Ala-Pro- and Gln-Lys-β-*p*NA with 105, -5 and -33, respectively). Thus, the principle that the hydrophobicity of the dipeptide portion determines the cleavability may be applicable to those substrates, except for Lys-Ile-(H.I. = 76), which is cleavable, and Trp-His- (H.I. = 105), which is not cleavable.

Three-dimensional structures of the S46 family members DPP7 and DPP11 are yet to be established. To date the structures of DPPs have been thoroughly determined in human DPPIII [29] that belongs to the metallopeptidase family M49 [16] and in human DPP7 [30] that belongs to the S28 DPPII family primarily specific for Pro. The present and previous studies [15,18] demonstrated that Phe664 and Gly666 of *P. gingivalis* DPP7/Phe671 and Arg673 of DPP11 are responsible for P2- and P1-position substrate recognition, respectively. Therefore, the three-dimensional model of DPP7 and DPP11 (Fig. 7) demonstrating adjacent locations of these residues to essential Ser is reasonably accepted.

If the presented models around essential Ser648 of DPP7 and Ser655 of DPP11 are appropriate, then Trp185 of GluV8, which is equivalent to Phe664 of DPP7, may also be involved in substrate recognition (Fig. 5A). It was previously shown that Trp185 of GluV8 is located adjacent to essential Ser169 and forms a substrate-binding pocket [25]. Moreover, W185Y substitution in GluV8, which naturally occurs in the GluV8-family member in *Staphylococcus epidermidis* [31], caused a reduction of the activity due to a 13.8-fold increase in the K_m value [32]. These findings also support the appropriateness of the model.

In conclusion, our results clarify the detailed substrate preference of DPP7 and DPP11 taking P2 preference into consideration, and further identified Phe664/Phe671 as residues participating in the S2 subsite of both DPPs. These findings expand current knowledge regarding the repertoire of peptide substrates managed by DPPs of *P. gingivalis*, and accordingly, by other proteolytic and asaccharolytic

bacteria expressing DPP7 and DPP11.

Acknowledgments

We greatly acknowledge M. Naito and H. Kondo for the fruitful discussions, and T. Kobayakawa (Nagasaki University) for the technical assistance. This work was supported by grants-in-aid for scientific research from the Ministry of Education, Science, Sports, and Culture of Japan (to Y.O.-N., S.K. and T.K.N.) and from the Institute for Fermentation, Osaka (to T.K.N.). S.M.A. Rouf is a graduate student supported by a Japanese Government (MEXT) Scholarship.

References

[1] Holt S.C., Ebersole J., Felton J., Brunsvold M., Kornman K.S. (1988) Implantation of *Bacteroides gingivalis* in nonhuman primates initiates progression of periodontitis. Science 239, 55–57.
[2] Lamont R.J., Jenkinson H.F. (1998) Life below the gum line: pathogenic mechanisms of *Porphyromonas gingivalis*. Microbiol. Mol. Biol. Rev. 62, 1244–1263.
[3] White D., Mayrand D. (1981) Association of oral Bacteroides with gingivitis and adult periodontitis. J. Periodontal Res. 16, 259–265.
[4] Moore W.E.C., Holdeman L.V., Smibert R.M., Good I.J., Burmeister J.A., Palcanis K.G. et al. (1982) Bacteriology of experimental gingivitis in young adult humans. Infect. Immun. 38, 651–667.
[5] Loesche W.J., Syed S.A., Schmidt E., Morrison E.C. (1985) Bacterial profiles of subgingival plaques in periodontitis. J. Periodontol. 56, 447–456.
[6] Hämäläinen P., Meurman J.H., Keskinen M., Heikkinen E. (2003) Relationship between dental health and 10-year mortality in a cohort of community-dwelling elderly people. Eur. J. Oral Sci. 111, 291–296.
[7] Iwai T., Inoue Y., Umeda M., Huang Y., Kurihara N., Koike M. et al. (2005) Oral bacteria in the occluded arteries of patients with Buerger disease. J. Vasc. Surg. 42, 107–115.
[8] Kshirsagar A.V., Offenbacher S., Moss K.L., Barros S.P., Beck J.D. (2007) Antibodies to periodontal organisms are associated with decreased kidney function. The dental atherosclerosis risk in communities study. Blood Purif. 25, 125–132.
[9] Detert J., Pischon N., Burmester G.R., Buttgereit F. (2010) The association between rheumatoid arthritis and periodontal disease. Arthritis Res. Ther. 12, 218.
[10] Citron D.M., Poxton I.R., Baron E.J. (2007) *Bacteroides*, *Porphyromonas*, *Prevotella*, *Fusobacterium*, and other anaerobic Gram-negative rods. In: P.R. Murray, E.J. Baron, J.H. Jorgensen, M.L. Landry, M.A. Pfaller (Eds.), Manual of Clinical Microbiology. ninth ed. Washington, D.C.: ASM Press, pp. 911–932.
[11] Takahashi N., Sato T., Yamada T. (2000) Metabolic pathways for cytotoxic end product formation from glutamate- and aspartate-containing peptides by *Porphyromonas gingivalis*. J. Bacteriol. 182, 4704–4710.
[12] Takahashi N., Sato T. (2001) Preferential utilization of dipeptides by *Porphyromonas gingivalis*. J. Dent. Res. 80, 1425–1429.
[13] Banbula A., Bugno M., Goldstein J., Yen J., Nelson D., Travis J. et al. (2000) Emerging family of proline-specific peptidases of *Porphyromonas gingivalis*: purification and characterization of serine dipeptidyl peptidase, a structural and functional homologue of mammalian prolyl dipeptidyl peptidase IV. Infect. Immun. 68, 1176–1182.
[14] Banbula A., Yen J., Oleksy A., Mak P., Bugno M., Travis J. et al. (2001) *Porphyromonas gingivalis* DPP-7 represents a novel type of dipeptidylpeptidase. J. Biol. Chem. 276, 6299–6305.
[15] Ohara-Nemoto Y., Shimoyama Y., Kimura S., Kon A., Haraga H., Ono T. et al. (2011) Asp- and Glu-specific novel dipeptidyl peptidase 11 of *Porphyromonas gingivalis* ensures utilization of proteinaceous energy sources. J. Biol. Chem. 286, 38115–38127.
[16] Rawlings N.D., Barrett A.J., Bateman A. (2010) MEROPS: the peptidase database. Nucleic Acids Res. 38, D227–D233.
[17] Mentlein R., Gallwitz B., Schmidt W.E. (1993) Dipeptidyl-peptidase IV hydrolyses gastric inhibitory polypeptide, glucagon-like peptide-1(7–36)amide, peptide histidine methionine and is responsible for their degradation in human serum. Eur. J. Biochem. 214, 829–835.
[18] Rouf S.M.A., Ohara-Nemoto Y., Hoshino T., Fujiwara T., Ono T., Nemoto T.K. (2013) Discrimination based on Gly and Arg/Ser at Position 673 between dipeptidyl-peptidase (DPP) 7 and DPP11, widely distributed DPPs in pathogenic and environmental Gram-negative bacteria. Biochimie 95, 824–832.
[19] Naito M., Hirakawa H., Yamashita A., Ohara N., Shoji M., Yukitake H. et al. (2008) Determination of the genome sequence of *Porphyromonas gingivalis* strain ATCC 33277 and genomic comparison with strain W83 revealed extensive genome rearrangements in *P. gingivalis*. DNA Res. 15, 215–225.
[20] Barret A.J., Chen J.-M. (2013) Dipeptidyl-peptidase III. In: N.D. Rawlings, G. Salvesen (Eds.), Handbook of Proteolytic Enzymes. third ed. Washington, D.C.: ASM Press, pp. 1285–1289.
[21] Vukelić B., Salopek-Sondi B., Spoljarić J., Sabljić I., Meštrović N., Agić D. et al. (2012) Reactive cysteine in the active-site motif of *Bacteroides thetaiotaomicron* dipeptidyl peptidase III is a regulatory residue for enzyme activity. Biol. Chem. 393, 37–46.
[22] Nemoto T.K., Ono T., Ohara-Nemoto Y., Shimoyama Y., Kimura S., Takagi T. (2008) Characterization of the glutamyl endopeptidase from *Staphylococcus aureus* expressed in *Escherichia coli*. FEBS J. 275, 573–587.
[23] Ikeda Y., Ohara-Nemoto Y., Kimura S., Ishibashi K., Kikuchi K. (2004) PCR-based identification of *Staphylococcus epidermidis* targeting *gseA* encoding the glutamic-acid-specific protease. Can. J. Microbiol. 50, 493–498.
[24] Lambert C., Leonard N., de Bolle X., Depiereux E. (2002) ESyPred3D: Prediction of proteins 3D structures. Bioinformatics 18, 1250–1256.
[25] Prasad L., Leduc Y., Hayakawa K., Delbaere L.T. (2004) The structure of a universally employed enzyme: V8 protease from *Staphylococcus aureus*. Acta Cryst. D60, 256–259.
[26] Monera O.D., Sereda T.J., Zhou N.E., Kay C.M., Hodges R.S. (1995) Relationship of sidechain hydrophobicity and alpha-helical propensity on the stability of the single-stranded amphipathic α-helix. J. Pept. Sci. 1, 319–329.
[27] Carmona C., Gray G.L. (1987) Nucleotide sequence of the serine protease gene of *Staphylococcus aureus*, strain V8. Nucleic Acids Res. 15, 6757.
[28] Potempa J., Banbula A., Travis J. (2013) Dipeptidyl-peptidase 7 of *Porphyromonas gingivalis*. In: N.D. Rawlings, G. Salvesen (Eds.), Handbook of Proteolytic Enzymes. third ed. Washington, D.C.: ASM Press, pp. 3641–3643.
[29] Bezerra G.A., Dobrovetsky E., Viertlmayr R., Dong A., Binter A., Abramic M. et al. (2012) Entropy-driven binding of opioid peptides induces a large domain motion in human dipeptidyl peptidase III. Proc. Natl. Acad. Sci. USA 109, 6525–6530.
[30] Bezerra G.A., Dobrovetsky E., Dong A., Seitova A., Crombett L., Shewchuk L.M. et al. (2012) Structures of human DPP7 reveal the molecular basis of specific inhibition and the architectural diversity of proline-specific peptidases. PLoS One 7, e43019.
[31] Ohara-Nemoto Y., Ikeda Y., Kobayashi M., Sasaki M., Tajika S., Kimura S. (2002) Characterization and molecular cloning of a glutamyl endopeptidase from *Staphylococcus epidermidis*. Microbiol. Pathog. 33, 33–41.
[32] Nemoto T.K., Ono T., Shimoyama Y., Kimura S., Ohara-Nemoto Y. (2009) Determination of three amino acids causing alteration of proteolytic activities of staphylococcal glutamyl endopeptidases. Biol. Chem. 390, 277–285.